

Fiber based polarization filter for radially and azimuthally polarized light

Christoph Jocher,^{1,*} Cesar Jauregui,¹ Christian Voigtländer,¹ Fabian Stutzki,¹
Stefan Nolte,¹ Jens Limpert,^{1,2} and Andreas Tünnermann^{1,2,3}

¹Friedrich-Schiller-Universität Jena, Institute of Applied Physics, Albert-Einstein-Str. 15, 07745 Jena, Germany

²Helmholtz-Institute Jena, Helmholtzweg 4, 07743 Jena, Germany

³Fraunhofer Institute for Applied Optics and Precision Engineering, Albert-Einstein-Str. 7, 07745 Jena, Germany

*christoph.jocher@uni-jena.de

Abstract: We demonstrate a new fiber based concept to filter azimuthally or radially polarized light. This concept is based on the lifting of the modal degeneracy that takes place in high numerical aperture fibers. In such fibers, the radially and azimuthally polarized modes can be spectrally separated using a fiber Bragg grating. As a proof of principle, we filter azimuthally polarized light in a commercially available fiber in which a fiber Bragg grating has been written by a femtosecond pulsed laser.

©2011 Optical Society of America

OCIS codes: (060.2310) Fiber optics; (060.2400) Fiber properties; (060.2280) Fiber design and fabrication; (060.2420) Fibers, polarization-maintaining; (060.3735) Fiber Bragg gratings.

References and links

1. V. G. Niziev and A. V. Nesterov, "Influence of beam polarization on laser cutting efficiency," *J. Phys. D Appl. Phys.* **32**(13), 1455–1461 (1999).
2. L. Novotny, M. R. Beversluis, K. S. Youngworth, and T. G. Brown, "Longitudinal field modes probed by single molecules," *Phys. Rev. Lett.* **86**(23), 5251–5254 (2001).
3. Q. Zhan, "Evanescence Bessel beam generation via surface plasmon resonance excitation by a radially polarized beam," *Opt. Lett.* **31**(11), 1726–1728 (2006).
4. Q. Zhan, "Trapping metallic Rayleigh particles with radial polarization," *Opt. Express* **12**(15), 3377–3382 (2004).
5. W. D. Kimura, G. H. Kim, R. D. Romea, L. C. Steinhauer, I. V. Pogorelsky, K. P. Kusche, R. C. Fernow, X. Wang, and Y. Liu, "Laser acceleration of relativistic electrons using the inverse Cherenkov effect," *Phys. Rev. Lett.* **74**(4), 546–549 (1995).
6. M. Stalder and M. Schadt, "Linearly polarized light with axial symmetry generated by liquid-crystal polarization converters," *Opt. Lett.* **21**(23), 1948–1950 (1996).
7. R. Dorn, S. Quabis, and G. Leuchs, "Sharper focus for a radially polarized light beam," *Phys. Rev. Lett.* **91**(23), 233901 (2003).
8. S. C. Tidwell, D. H. Ford, and W. D. Kimura, "Generating radially polarized beams interferometrically," *Appl. Opt.* **29**(15), 2234–2239 (1990).
9. T. G. Euser, M. A. Schmidt, N. Y. Joly, C. Gabriel, C. Marquardt, L. Y. Zang, M. Förtsch, P. Banzer, A. Brenn, D. Elser, M. Scharrer, G. Leuchs, and P. St. J. Russell, "Birefringence and dispersion of cylindrically polarized modes in nanobore photonic crystal fiber," *J. Opt. Soc. Am. B* **28**(1), 193–198 (2011).
10. S. Ramachandran, P. Kristensen, and M. F. Yan, "Generation and propagation of radially polarized beams in optical fibers," *Opt. Lett.* **34**(16), 2525–2527 (2009).
11. F. Stutzki, C. Jauregui, C. Voigtländer, J. U. Thomas, J. Limpert, S. Nolte, and A. Tünnermann, "Passively stabilized 215 W monolithic CW LMA-fiber laser with innovative transversal mode filter," *Proc. SPIE* **7580**, 75801K, 75801K-10 (2010).
12. F. Stutzki, C. Jauregui, J. Limpert, and A. Tünnermann, "Real-time characterisation of modal content in monolithic few-mode fiber lasers," *Electron. Lett.* **47**(4), 274–275 (2011).
13. J. M. O. Daniel, J. S. P. Chan, J. W. Kim, J. K. Sahu, M. Ibsen, and W. A. Clarkson, "Novel technique for mode selection in a multimode fiber laser," *Opt. Express* **19**(13), 12434–12439 (2011).
14. A. W. Snyder, "Asymptotic expressions for eigenfunctions and eigenvalues of a dielectric or optical waveguide," *IEEE Trans. Microw. Theory Tech.* **17**(12), 1130–1138 (1969).
15. D. Gloge, "Weakly guiding fibers," *Appl. Opt.* **10**(10), 2252–2258 (1971).
16. A. W. Snyder and J. D. Love, *Optical Waveguide Theory* (Kluwer Academic, 1983).
17. T. Erdogan, "Fiber grating spectra," *J. Lightwave Technol.* **15**(8), 1277–1294 (1997).
18. J. U. Thomas, C. Voigtländer, S. Nolte, A. Tünnermann, N. Jovanovic, G. D. Marshall, M. J. Withford, and M. Steel, "Mode selective fibre Bragg grating," *Proc. SPIE* **7589**, 75890J, 75890J-9 (2010).

1. Introduction

Azimuthally and radially polarized beams have attracted significant attention recently. The reasons for this interest are to be found in the wide application field of these polarizations, which include efficient material processing [1], microscopy [2], excitation of plasmons [3], optical trapping [4] and electron acceleration [5]. A stable source with high polarization purity is required for these applications. The common approach to generate azimuthally and radially polarized beams is based on converters, which transform a linearly polarized beam in these polarization states. Three converter types are often used: liquid-crystal-based polarization converters [6], segmented half-wave plates [7], and interferometric setups [8]. The disadvantage of these methods is the sophisticated experimental setup with their free-space beam propagation that makes them sensitive to misalignments which negatively affect the polarization purity of the converted light.

Although optical waveguides, and fibers in particular, are in principle suitable for guiding, converting and generating azimuthally and radially polarized modes, there are only a few methods proposed up to now to carry out this task. Generally, fibers can guide azimuthally and radially polarized light, but their polarization is not maintained in every fiber. The best maintenance of the polarization is possible when fibers with strongly lifted modal degeneracy are used. This can be achieved, for example, using a photonic crystal fiber with a very small core and a large ratio between hole-diameter and hole-to-hole-distance (pitch) as proposed in [9]. Another possible approach for guiding and converting such polarizations is to employ a special fiber design [10]. Through a micro-bend grating and a polarization controller, an existing linearly polarized beam can be coupled from the core to a radially or azimuthally polarized beam, which is, in turn, guided in a surrounding ring structure.

Here we present a concept suitable for converting and generating azimuthally or radially polarized light that exploits the fact that the modal degeneracy is lifted in a strongly guiding fiber, such as, for example, a high NA step index fiber. This implies that in these waveguides the azimuthally and radially polarized fiber modes will exhibit different effective refractive indices. Thus, if the index difference between the modes is high enough, the modes can be spectrally separated by means of a narrowband fiber Bragg grating (FBG) in a similar fashion as what was done in [11–13] with weakly guiding fibers and, therefore, with linearly polarized modes.

The paper is organized as follows: in section 2 the theoretical background of strongly guiding optical fibers (i.e. fibers with lifted modal degeneracy) is briefly reviewed. Additionally, the conditions required to filter radially or azimuthally polarized light using a FBG are presented in that section. In section 3 the experimental setup used for the proof of principle is described and the results are presented. Finally, some conclusions are drawn.

2. Theory

2.1 Strongly guiding optical fibers

Many optical fiber designs pursue single-mode operation. In step index fibers strictly single-mode designs are possible if the NA of the fiber for a fixed core diameter is low enough. This type of fiber is by far the most widely used and they belong to the category generically known as weakly guiding fiber designs [14,15]. It is worth noting that even though weakly guiding fibers are always characterized by a small difference between the indices of refraction of the core and the cladding, they do not necessarily have to be single-mode. Generally the modal properties of fibers are characterized by the V-parameter, calculated with the core radius, the wavelength and the NA. This way, a fiber can guide higher order modes (HOMs) for V-parameters larger than 2.405.

An important characteristic of the weakly guiding fibers which have been preferentially used in the last decade is that many HOMs are degenerated (i.e. they share the same intensity

profile and have nearly identical effective indices) [14]. In practice this means that they cannot be individually excited with conventional means (or only with extreme difficulty), and only a degenerated mode formed by the overlap of several HOMs will be observed. As shown in [15] these degenerated modes are, in a first approximation, linearly polarized. Because of this characteristic, i.e. their state of polarization, the modes of weakly guiding fibers are called linearly polarized (LP)-Modes [15]. However, it can be demonstrated that cylindrical waveguides support the propagation of other polarization states in HOMs, such as the radially and azimuthally polarized modes [16]. Thus, in cylindrical optical fibers one group of interesting HOMs sharing a similar intensity profile are the TE_{01} , TM_{01} and two HE_{21} modes. The TE_{01} and the TM_{01} being particularly interesting, because they intrinsically show outstanding polarization characteristics: they are azimuthally (TE_{01}) and radially (TM_{01}) polarized, respectively, as seen in Fig. 1. However, if the optical fiber has a low NA, these interesting modes are guided with nearly the same effective refractive index, i.e. they are degenerated. Consequently, as mentioned before they cannot be individually excited using conventional techniques and, additionally, mode coupling can easily occur at any imperfection and, as a result, the observed mode is predominantly linearly polarized and not radially or azimuthally any more.

On the other hand, it can be demonstrated that in fibers with a high NA (also known as strongly guiding fibers) the modal degeneracy is lifted [16]. Thus, in our example, the TE_{01} , TM_{01} and two HE_{21} modes will have different effective refractive indices at almost any given wavelength. Consequently, mode coupling is drastically reduced, the modes can be individually excited and, additionally, the TE_{01} and TM_{01} modes maintain their polarization during propagation. The intensity patterns together with the polarization directions for the TE_{01} , TM_{01} and two HE_{21} modes and the corresponding degenerated modes, i.e. the LP_{11} modes, are shown in Fig. 1.

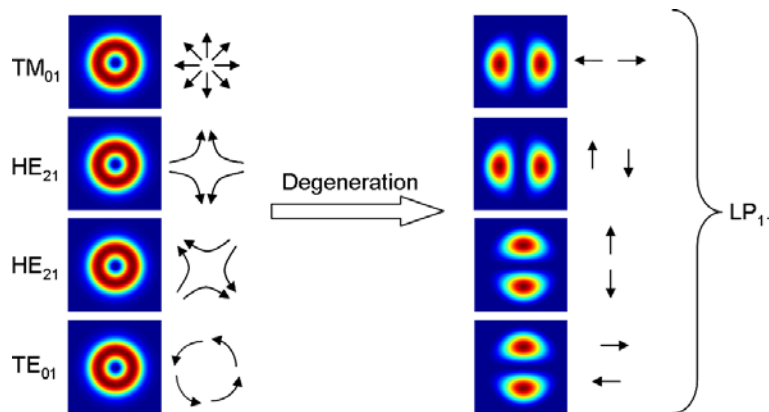


Fig. 1. Intensity patterns together with the intrinsic polarization characteristics for the TE_{01} , TM_{01} and two HE_{21} modes. In weakly guiding fibers this set of modes is degenerated giving rise to the LP_{11} -modes, which are shown on the right-hand side.

The differences in effective refractive index between the TE_{01} , TM_{01} and the two HE_{21} modes in a strongly guiding step index fiber when varying the NA (from 0.35 to 0.65) and the core size (radius ranging from 0.5 to 4 μm) have been numerically calculated for a wavelength of 1030 nm. Figure 2 (a) shows the effective index difference between the azimuthally polarized TE_{01} mode and its nearest neighbor in logarithmic scale (base 10). It should be noted that the “nearest neighbor” denomination can refer to different modes, as in some cases the TM_{01} has a higher effective refractive index than the two quasi-degenerated HE_{21} modes and vice-versa. In Fig. 2 (b), on the other hand, the absolute value of the effective index difference between the TM_{01} and the two almost degenerated HE_{21} modes is shown. It should be mentioned that this difference is negative for fibers operating near the single mode region (represented by the white areas in Fig. 2), which implies that the TM_{01} mode has a higher

effective index than the HE_{21} modes. Additionally, for some combinations of NA and core size the TM_{01} mode becomes degenerated with the two HE_{21} modes, a situation that is indicated by a zero distance (dark blue stripe) between these modes in Fig. 2 (b).

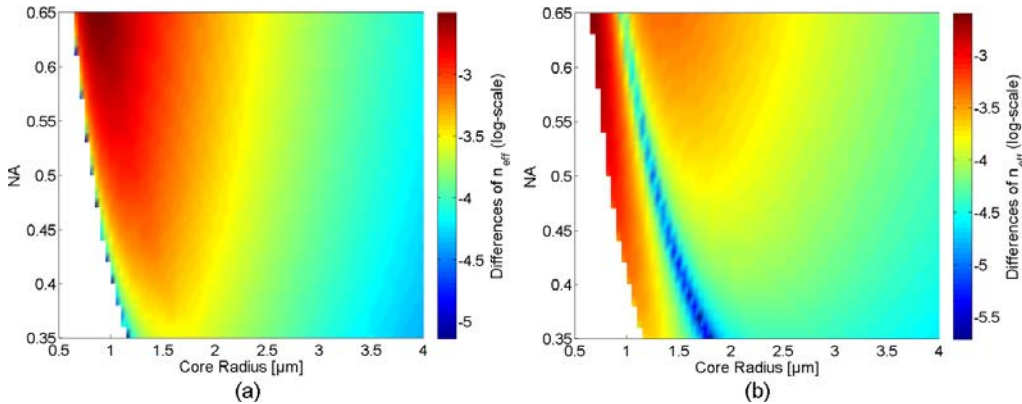


Fig. 2. Effective index difference (a) between the TE_{01} and its nearest neighbor mode and (b) between the TM_{01} and the two HE_{21} modes in a strongly guiding step index fiber as a function of the core radius and the NA, shown in logarithmic scale. The wavelength is 1030 nm.

The calculation also shows that the highest effective index separation for any given NA is not reached for the smallest core size. Additionally, if azimuthally and radially polarized beams should be filtered using the same fiber, this fiber should lift the polarization degeneracy in such a degree that these two modes exhibit a large separation in effective index to one another and to the other modes. Thus, the optimum fiber core radius can be read from Fig. 2 for any given NA.

From the figure above it is clear that in order to filter an azimuthally and/or radially polarized beam a fiber with a higher NA is more suitable than a fiber with a lower NA. Furthermore, smaller cores are normally advantageous (provided that they are not too small). Such high NA small core fibers are commercially available since they are widely used for enhancing non-linear effects, e.g. for supercontinuum generation.

Figure 3 shows the simulated lifting of the modal degeneracy in one of these step-index ultra-high NA fibers with a 1.5 μm core radius and 0.41 NA as a function of the wavelength. Only the differences between the effective indices of the TE_{01} (blue line) and the TM_{01} (red line) modes to the HE_{21} modes are shown. It is worth mentioning, though, that for this calculation the fiber NA is considered to remain constant with the wavelength. This has been done because the material properties of the fiber are not known. Even though in reality the NA of the fiber will most certainly not remain constant with wavelength, this will only shift the features of Fig. 3 but it should not alter the trends revealed by it. Thus, from Fig. 3 it is clear that for this fiber there are some particularly interesting regions with a highly lifted mode degeneracy for the azimuthally or radially polarized beams. One of these regions is situated around 1365 nm, it is characterized by all the modes (TE_{01} , TM_{01} and HE_{21}) being equidistant. Moreover, at this particular wavelength the effective index differences between neighboring modes are larger than at any other wavelength. Another interesting region is found below 1000 nm, where the TM_{01} mode has the lowest effective index. Thus it can be concluded that Fig. 3 shows wide regions of lifted mode degeneracy in this fiber that can be used to filter radially and/or azimuthally polarized light. Unfortunately, exactly in the interesting spectral region around 1000 nm (where most high power fiber systems operate) the TM_{01} mode is degenerated with the two HE_{21} modes. This implies that with this fiber in this region it will only be possible to obtain azimuthally polarized light. It should be highlighted, though, that this limitation is fiber specific. Thus, other fiber designs will be able to provide a high lifting of the modal degeneracy around 1000nm.

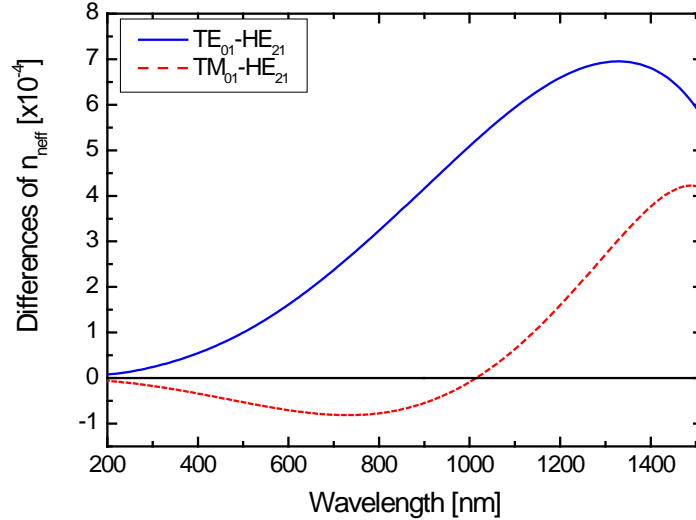


Fig. 3. Effective refractive index differences between the TE₀₁, TM₀₁ and HE₂₁ modes for a step-index fiber with a core diameter of 3 μm and a NA of 0,41 as a function of wavelength.

2.2 Filtering of radially and/or azimuthally polarized light using fiber Bragg gratings in strongly guiding fibers

A fiber Bragg grating (FBG) is a periodic or quasi-periodic modulation of the refractive index along the fiber. If the modulation period is Λ , a fiber mode with an effective refractive index n_{eff} and a wavelength λ will be reflected by the FBG in the diffraction order m , if the Bragg condition (1) is fulfilled [17]:

$$\lambda = 2 \cdot n_{eff} \cdot \frac{\Lambda}{m}. \quad (1)$$

Thus, the spectral separation $\Delta\lambda$ between the grating resonances corresponding to two transversal modes with effective refractive index $n_{eff,1}$ and $n_{eff,2}$ can be calculated by Eq. (2). This way, the FBG maps the effective index differences of all propagating modes into the spectrum:

$$\Delta\lambda = 2 \left(n_{eff,1} - n_{eff,2} \right) \frac{\Lambda}{m}. \quad (2)$$

Additionally, if two modes should be clearly separated, the reflection bandwidth of the FBG has to be smaller than the spectral separation between two adjacent grating resonances. Otherwise, if the reflection bandwidth is too large, the spectral wings of one grating resonance will overlap with the neighboring one and, therefore, the polarization purity of the reflected light will be reduced. In fact, the ideal situation is that the reflection bandwidth of the FBG is narrower than the spectral separation between the modes of interest. Thus, each mode is reflected at its own wavelength and they do not overlap. In this situation a radially or azimuthally polarized beam can be obtained by addressing the FBG with the appropriate wavelength (assuming that the corresponding mode has been excited at this wavelength). Of course the drawback is that the radially or azimuthally polarized modes have to exist in the fiber first in order to be reflected by the homogenous FBG. However, in a passive fiber this can be easily achieved by playing with the coupling optics (in free space setups) or by using, for example, offset splices. The expected stability and polarization purity offered by this approach is high, because only one mode is reflected at each wavelength.

One additional advantage of this FBG-based approach to filter radially or azimuthally polarized light is that the Bragg condition allows converting one mode into another at some specific wavelengths. However, in order to do this an inhomogeneous FBG is required [18].

For example the fundamental mode HE_{11} can be converted into a radially or azimuthally polarized mode. If the complete reflection spectrum is considered, the conversion peaks are spectrally equidistant to the resonances of the fundamental mode and to the resonance of their corresponding counterpart TE_{01} , TM_{01} or HE_{21} . However, this mode conversion is a two-way road, which implies that any radially or azimuthally polarized mode incident on the FBG will be converted into a linearly polarized fundamental mode. Therefore, for an efficient conversion it has to be ensured that only the fundamental mode is excited in the incoming direction.

3. Experiment

3.1 Experimental setup

For the proof of principle of this technique we use a commercially available step index high NA fiber (Nufern UHNA7). The cut-off wavelength of this fiber is 1470 nm and its core radius is $\sim 1.5 \mu\text{m}$. However, the most important parameter of this fiber is its very high NA, with a nominal value of 0.41. Thus, according to Fig. 2 or Fig. 3, it can be expected that in this fiber the effective index difference between the azimuthally polarized mode and its closest neighbor is 5.4×10^{-4} at a wavelength of 1030 nm. On the other hand, for the radially polarized mode this effective index difference is 8×10^{-6} . The fiber grating (FBG) was written using a femtosecond laser and the phase mask technique described in [19]. The FBG was 15 mm long with a uniform profile and had a photo-induced index change of around 1×10^{-3} (peak-to-peak). During the fabrication process the transmission spectrum of the fundamental mode was measured to obtain an estimation of the grating reflectivity, which was found to be ~ 23 dB. Taking into account that the period is 712.5 nm and in the setup its second diffraction order ($m = 2$ in Eq. (1)) is used, we can expect a spectral separation of 400 pm for the azimuthally polarized mode and 6 pm for the radially polarized one. As can be seen, and also as previously discussed, in this fiber it is not possible to fully resolve the radially polarized mode in this wavelength range since the bandwidth of the FBG is ~ 150 pm. As a proof of principle, though, it is still possible to filter the azimuthally polarized mode.

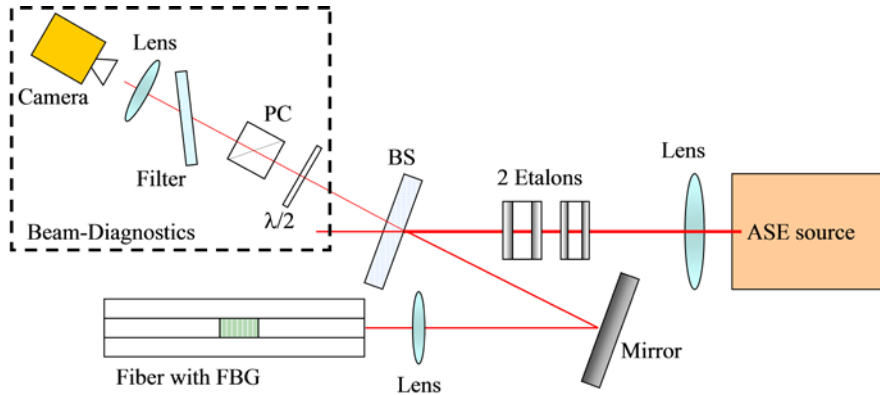


Fig. 4. Experimental setup used for the proof-of-principle filtering of an azimuthally polarized beam. PC: polarizing cube, BS: beam splitter.

The experimental setup is illustrated in Fig. 4. A home-made unpolarized single mode ASE source is used as the light source. It is coupled into the high-NA fiber using a polarization independent 50% dichroic beam splitter. In order to excite the azimuthally polarized beam, the focusing lens is purposefully misaligned. Two etalons selectively filter the ASE source leaving just a 0.2 nm bandwidth range around the desired resonance wavelength of the FBG. The beam reflected by the FBG is analyzed after the beam splitter, where a second dichroic band-pass filter with a transmission band of 10 nm is used to filter out spurious wavelengths coming from the spectrally periodic transfer function of the etalons.

The polarization is analyzed by using a polarization cube, a rotating half-wave plate and imaging the near-field on a camera.

3.2 Experimental results

In order to characterize the setup, the reflected spectrum from the FBG (without the etalons and the beam diagnostics part) is measured and shown in Fig. 5. The background level comes from a reflection from the ASE-source. The resonance at 1060.8 nm corresponds to the fundamental mode (HE_{11}), which was theoretically expected at 1059.7 nm. Similarly, the resonance at 1045.2 nm corresponds to the azimuthally polarized (TE_{01}) mode. The radially polarized (TM_{01}) and the two HE_{21} modes are represented by the reflection peak at 1044.4 nm. The mode conversion peaks are the group of resonances centered around 1052.8 nm. The presence of these mode conversion resonances indicate that the FBG is not transversally homogeneous over the core. By offsetting the coupling lens, the intensity distribution in the different reflection peaks can be changed, thus providing an indication of the coupling efficiency in any desired mode. Additionally, the double-peak that can be seen at the resonance corresponding to the fundamental mode (1060.8 nm) points out to a FBG-induced birefringence. This birefringence is not desirable since it may reduce the polarization purity of the azimuthally or radially polarized modes. It is worth mentioning at this point that this birefringence is not inherent to FBGs but it comes as a result of our FBG being too strong and transversally inhomogeneous (as revealed by the presence of the conversion peaks in the spectrum). It can be seen in Fig. 5 that the distance between the azimuthally and the radially or mixed polarized modes is 0.8 nm. This value is, as mentioned before, much higher than our simulation estimates (~ 0.4 nm). This discrepancy cannot be explained by fabrication tolerances of the fiber. Therefore, our hypothesis is that the guiding structure has been deeply altered by the fs-written FBG, which has resulted in a stronger lifting of the modal degeneracy in the fiber region comprising the FBG.

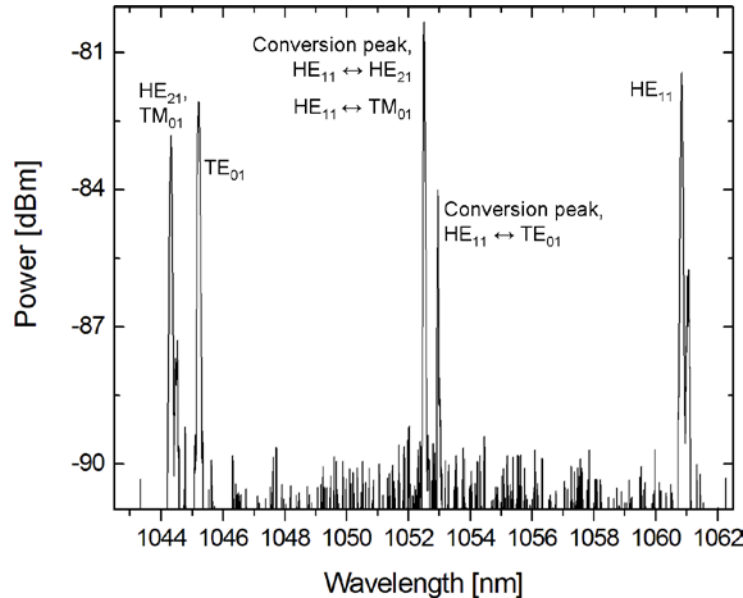


Fig. 5. Reflected spectrum of the FBG measured with an optical spectrum analyzer.

With the above described diagnostic setup, the reflection peaks coming from the FBG are individually spectrally filtered and analyzed. The modes TE_{01} and TM_{01} (and eventually even the HE_{21}) can be clearly identified using a camera and a polarizer. However, in discerning between modes, the transmission direction of the polarizer is of capital importance. The two lobes shown in Fig. 6 appear for each of these modes after going through the polarizer, but for

a TE_{01} the zero-intensity line separating the lobes should be oriented parallel to the transmission direction of the polarizer (transmission direction indicated by the white arrows in Fig. 6). On the other hand, for a TM_{01} that zero-intensity line should be oriented orthogonal to the transmission direction of the polarization cube. Additionally, if the half-wave plate is turned, the rotation direction of the two lobes helps to distinguish between the TE_{01}/TM_{01} (they rotate in the direction of the half-wave plate) modes and the HE_{21} modes (they rotate in the opposite direction of the half-wave plate). In the paper the measured beam shows all the characteristics of a TE_{01} mode. Figure 6 shows the theoretically expected azimuthally polarized beam for this fiber (above) together with the experimental measurement at 1045.2 nm (below). The column (a) in Fig. 6 illustrates the full intensity pattern of the azimuthally polarized mode. Without any polarization analysis, it exhibits the characteristic doughnut shape. In Fig. 6 column (b-e) the results of the polarization analysis with different transmission directions of the polarizer (indicated by the white arrows) is shown in false-color. It should be pointed out that all the false-color pictures have been normalized to the maximum intensity of column (a). A video obtained by rotating the half-wave plate can also be seen in [Media 1](#). It is worth mentioning that in this setup, due to the mentioned birefringence of the FBG, no perfectly azimuthally polarized beam could be filtered. This explains the non-perfectly symmetric polarization results shown in Figs. 6 (c) and (e). Additionally, the polarization of the analyzed beam is further affected by the dichroic beam splitter used (which exhibits a slight polarization dependence). The impact of these effects is particularly clear in Fig. 6 (e), which shows a nearly linearly polarized doughnut shape. In spite of these experimental caveats, it can be seen that the polarization purity of the azimuthally polarized beam is reasonably high. In future work we expect to overcome the described problems and to further enhance the polarization purity.

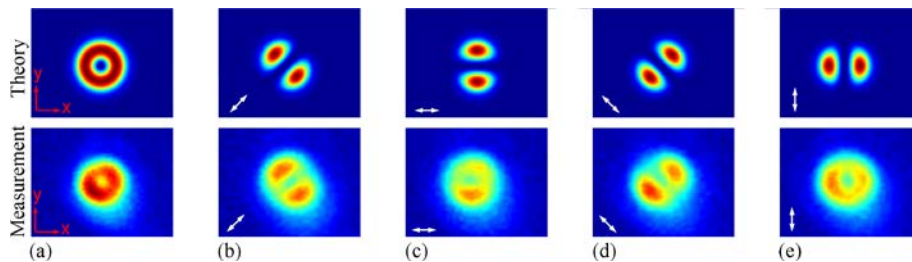


Fig. 6. Theoretical azimuthally polarized beam (above) together with the corresponding measurement (below) at 1045.2 nm. (a) Intensity distribution without PC and half-wave plate. (b-e) Polarization filtered beam with the PC and half-wave plate at different transmission directions as indicated by the arrow. A video showing the rotation of the polarization filtered beam with the half-wave plate is presented in [Media 1](#).

4. Conclusion

In conclusion we have presented a new fiber based mode filter for azimuthally and radially polarized light. This simple concept uses only a strongly guiding fiber with a FBG. Therefore, this approach makes compact all-fiber setups possible.

The lifting of the modal degeneracy in strongly guiding fibers has been simulated at 1030 nm and its dependence on different core diameters and NAs has been analyzed. It has also been shown that a narrowband FBG in a strongly guiding fiber can lead to the spectral separation of the azimuthally and radially polarized modes.

This concept has been experimentally verified in a proof-of-principle experiment that uses a commercially available strongly guiding fiber. In this setup the azimuthally polarized mode has been successfully separated. The results of this proof-of-principle experiment are very encouraging.

The proposed technique can theoretically generate radially or azimuthally polarized light with very high polarization purity. This concept is in essence a modal filter that can be easily

integrated in a fiber laser cavity to build an azimuthally or radially polarized all-fiber oscillator.

Acknowledgments

We acknowledge financial support by the German Federal Ministry of Education and Research (BMBF) under contract No. 13N9687 and the German Research Foundation (DFG) within the Leibniz program.